Conformational Analysis of the Cyclised Pyridoxal Schiff Base of L-Tryptophan. X-Ray Crystal Structure, Nuclear Magnetic Resonance and Molecular Orbital Studies of 3-Carboxy-1-{3-hydroxy-2-methyl-5-[(phosphonooxy)methyl]-4-pyridyl}-1,2,3,4-tetrahydro-β-carboline

Hiroomi Nagata,[a] Mitsunobu Doi,[a] Masatoshi Inoue,[a] Toshimasa Ishida,*[,a] Miyoko Kamigauchi,[b] Makiko Sugiura[b] and Akio Wakahara[c]

[a] *Department of Physical Chemistry, Osaka University of Pharmaceutical Sciences, 2-10-65 Kawai, Matsubara, Osaka 580, Japan*

[b] *Kobe Women's College of Pharmacy, 4-19-1 Motoyamakita-machi, Higashinada-ku, Kobe 658, Japan*

[c] *Fujisawa Pharmaceutical Co. Ltd., 2-1-6 Kashima, Yodogawa-ku, Osaka 532, Japan*

In order to deduce the structural features of cyclised Schiff bases in their *in vivo* regulation of pyridoxal-requiring enzymes, the molecular conformation of 3-carboxy-1-{3-hydroxy-2-methyl-5-[(phosphonooxy)methyl]-4-pyridyl}-1,2,3,4-tetrahydro-β-carboline, a cyclised Schiff base between pyridoxal 5-phosphate and L-tryptophan, has been investigated by X-ray crystal analysis, ^{1}H NMR measurements and molecular orbital calculations. In the crystalline state the molecule, which is in a double zwitterionic state with the hydroxy and phosphate oxygen atoms deprotonated and the pyridine and β-carboline nitrogen atoms protonated, takes a rigid conformation stabilized by two intramolecular hydrogen bonds between the carboline NH and pyridoxal O^- and between the indole NH and phosphate O^- atoms. This solid conformation also appears to be the preferred conformation in DMSO solution, as judged from appreciable ROEs between protons and *J* values. Conformational analysis by CNDO/2 calculations showed the conformation observed in the crystal also to be energetically the most favourable. The importance of this molecular conformation for the biological function of the cyclised Schiff base is discussed.

Pyridoxal 5-phosphate (PLP) plays not only an important physiological function as vitamin B6, but also is an essential co-factor for various enzymes which catalyse metabolic reactions of amino acids such as decarboxylation, racemization, trans-amination and Cα–Cβ bond cleavage.[1] In the metabolic reactions of amino acids, PLP forms a Schiff base with the amino acid as a key intermediate, which is believed to be transformed into the end product according to Dunathan's hypothesis.[2] However, it is known that the PLP Schiff bases of some amino acids such as histidine and tryptophan[3,4] further undergo cyclisation to form the tetrahydropyrido derivatives under physiological conditions without enzymatic participation, and these cyclic compounds can be thought of as *in vivo* regulators for controlling the metabolism of amino acids, since they inhibit the activity of PLP-requiring enzymes.[5–10]

Tryptophan plays an important role in nature not only by serving as a building block or functional unit in proteins, but also by taking part in the biosyntheses of hormones and neurotransmitters. In the metabolic pathway of tryptophan, the transformation of tryptophan to tryptamine, 5-hydroxytryptophan to serotonin, serotonin to 5-hydroxyindoleacetate and tryptamine to indoleacetate are catalysed by PLP-requiring enzymes (aromatic L-amino acid decarboxylase or monoamine oxidase). Since the cyclisation of their PLP Schiff bases could play a regulatory role in enzymatic reactions of these tryptophan metabolites,[9–11] information on stereostructural features of these cyclised products should be useful for elucidating the *in vivo* feedback mechanism controlling the metabolism of tryptophan and for elucidating the substrate-specificity of the PLP-requiring enzyme.

In this paper, we present the conformational analysis of a cyclised PLP Schiff base of L-tryptophan, *i.e.* 3-carboxy-1-{3-hydroxy-2-methyl-5-[(phosphonooxy)methyl]-4-pyridyl}-1,2,3,4-tetrahydro-β-carboline **1** (Fig. 1), studied by X-ray single crystal analysis, ^{1}H NMR measurements and molecular orbital calculations. Although structural data on synthetic tetrahydrocarboline derivatives have been reported previously,[12–14] there is no example of a naturally occurring compound in which the pyridoxal coenzyme is incorporated.

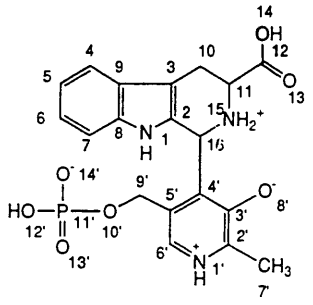

1

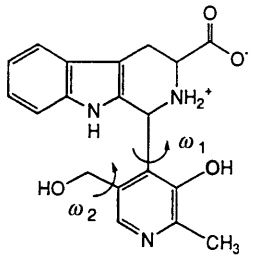

2

Fig. 1 Chemical structures of **1** and **2**, together with atomic numbering used for **1** in this paper

Table 1 Summary of crystal data and intensity collection details

Formula	$C_{19}H_{20}N_3O_7P\cdot(51/3)H_2O$
M_r	487.402
Crystal system	Trigonal
Space group	$R3$
a, b/Å	37.302(5)
c/Å	4.728(5)
V/Å^3	5697.3(6)
Z	9
D_m/g cm^{-3}	1.378(3)
D_x/g cm^{-3}	1.389
μ(Cu-Kα)/cm^{-1}	15.33
F(000)	2514
T of data collection/°C	18
Scan speed in 2θ/° min^{-1}	4
Scan range in ω/°	1.26 + 0.15 tan θ
Data range measured	$-44 \leqslant h \leqslant 44, 0 \leqslant k \leqslant 44,$ $0 \leqslant l \leqslant 6 (h + k \geqslant 0)$
No. of unique data measured	2418
No. of data used for refinement	2085 for $F_o \geqslant 3\sigma(F_o)$
No. of variables	135
R	0.0599
R_w	0.0626
S	0.8751

Experimental

Preparation of Single Crystals of **1**.—A mixture of aqueous solutions of equimolar (1 mmol dm^{-3}) PLP and L-tryptophan (free forms) was stirred for 1 h at 50 ~ 55 °C. The solution was then cooled slowly to room temperature (20 °C). Yellowish needle crystals were obtained by slow vapour diffusion after a few weeks.

X-Ray Crystal Data Collection.—A single crystal with dimensions of 0.1 × 0.1 × 0.4 mm was sealed in a glass capillary with some of the mother liquor. All X-ray measurements were made on a Rigaku AFC7R diffractometer with graphite monochromated Cu-Kα radiation (λ = 1.5418 Å) and a 12 kW rotating anode generator. Details of crystal data and intensity data collections are summarized in Table 1. Unit-cell dimensions were determined by a least-squares refinement using the setting angles of 25 carefully centred reflections in the range of 35 < 2θ < 45°. Crystal density was measured by the flotation method using a C_6H_6–CCl_4 mixture. Judging from the symmetry of cell dimensions ($a = b$, $\alpha = \beta = 90°$, $\gamma = 120°$) and from the condition limiting possible reflections [$-h + k + l = 3n$ for (hkl)], the space group was determined to be $R3$ with hexagonal axis. X-Ray reflectional intensities were collected using an ω-2θ scan technique to a maximum 2θ value of < 130 °. The weak reflections [$F_o < 3\sigma(F_o)$] were rescanned to ensure good counting statistics. Stationary background counts were recorded on each side of the reflections. Four standard reflections were monitored for every 100 reflection intervals and showed no significant time dependence. An empirical absorption correction using the DIFABS program[15] was applied, which resulted in transmission factors ranging from 0.88 to 1.15. The data were corrected for Lorentz and polarization effects.

Structure Solution and Refinement.—The structure was solved by direct methods using the MULTAN87 program.[16] All water molecules of crystallization were located by successive Fourier syntheses, in which a water molecule [O(6)W] was located on a three-fold axis with an occupancy of 1/3. The non-hydrogen atoms were refined anisotropically by full-matrix least-squares methods using the SHELX76 program.[17] The positions of the hydrogen atoms were obtained from the difference Fourier map and were included isotropically in the calculation of $|F_c|$ values, but not refined. The function of $\Sigma w(|F_o| - |F_c|)^2$ was minimized; in the final refinement, $w = 1/[\sigma(F_o)^2 + 0.006\,438|F_o|^2]$ was used. The maximum and minimum peaks on the final difference Fourier map corresponded to 0.21 and −0.27 e Å^{-3}, respectively. For all crystallographic calculations, the UNICS system[18] was used, and the atomic scattering factors and terms of anomalous dispersion corrections were taken from the literature.[19] Atomic coordinates, bond lengths and angles, and thermal parameters have been deposited at the Cambridge Crystallographic Data Centre.*

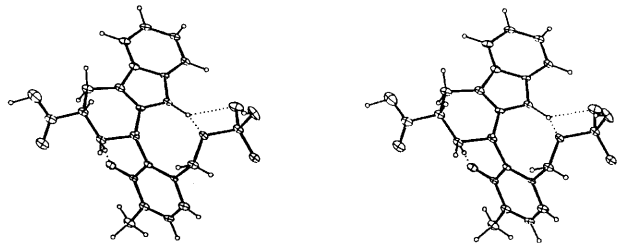

Fig. 2 Stereoscopic view of **1**. Dotted lines represent hydrogen bonds.

NMR Measurements.—The ^{1}H NMR measurements were carried out at a low concentration (*ca.* 3 mg cm^{-3}) in [$^2H_6$]dimethyl sulfoxide ([$^2H_6$]DMSO) solution. All NMR spectra were measured on a Varian VXR-500 spectrometer at 24 °C. The deuterium resonance of the solvent was used as the lock signal, and the chemical shifts were measured with respect to an internal reference of TMS (tetramethylsilane). Signal assignment was performed by two-dimensional correlated spectroscopy (COSY). The rotating frame Overhauser effect spectra (ROESY) were recorded in the phase-sensitive mode.

Molecular Orbital Calculations.—The most stable conformation of **1** was investigated by the use of CNDO/2 energy calculations on 3-carboxy-1-(3-hydroxy-5-hydroxymethyl-2-methyl-4-pyridyl)-1,2,3,4-tetrahydro-β-carboline **2** as a function of torsion angles around the C(2)–C(16)–C(4′)–C(5′) (ω_1) and C(4′)–C(5′)–C(9′)–O(10′) (ω_2) bonds. Compound **2** is a cyclised Schiff base of pyridoxal with L-tryptophan and was used to investigate the intrinsic stability of the orientation between the β-carboline ring and the PLP pyridine ring, *i.e.* to elucidate the importance of an N(15)H ··· O(8′) intramolecular hydrogen bond for characterizing the rigid conformation of **1**. The effect of external factors such as the N(1)H ··· O(14′) intramolecular hydrogen bond can be excluded by using compound **2** for the calculations. The chemical structure of **2** was treated as neutral with N(15) protonated and O(8′) deprotonated. The total energies of 144 different conformers were computed in increments of 30° of ω_1 and ω_2 torsion angles from 0 to 360°.

Results and Discussion

Molecular Conformation of **1**.—*Crystal conformation*. A stereoscopic view of the molecular conformation of **1** observed in the crystal structure is shown in Fig. 2. Selected torsion angles are given in Table 2. Because the interface between **1** and the water molecules of crystallization (discussed later) has less well formed crystallinity, the bond lengths and angles of **1** are not as accurate as usual. However, these values are all in the acceptable range, and no notable abnormality was observed. Electron densities corresponding to hydrogen atoms, which were revealed in a difference Fourier map, showed that **1** takes a

* For details of the deposition scheme, see 'Instructions for Authors,' *J. Chem. Soc., Perkin Trans. 2*, 1994, Issue 1.

Table 2 Selected torsion angles with their esds in parentheses

C(16)–C(2)–C(3)–C(10)	1.3(6)
C(2)–C(3)–C(10)–C(11)	13.1(5)
C(3)–C(10)–C(11)–N(15)	−42.6(5)
C(10)–C(11)–N(15)–C(16)	62.3(5)
C(11)–N(15)–C(16)–C(2)	−44.8(5)
C(3)–C(2)–C(16)–N(15)	13.8(4)
C(10)–C(11)–C(12)–O(13)	117.3(9)
C(10)–C(11)–C(12)–O(14)	−62.0(7)
N(15)–C(11)–C(12)–O(13)	−6.3(8)
N(15)–C(11)–C(12)–O(14)	174.3(7)
C(2)–C(16)–C(4′)–C(3′)	−76.2(5)
C(2)–C(16)–C(4′)–C(5′):ω_1	105.9(5)
N(15)–C(16)–C(4′)–C(3′)	43.6(5)
N(15)–C(16)–C(4′)–C(5′)	−134.4(5)
C(4′)–C(5′)–C(9′)–O(10′):ω_2	−58.9(5)
C(6′)–C(5′)–C(9′)–O(10′)	119.7(6)
C(5′)–C(9′)–O(10′)–P(11′)	−106.2(4)
C(9′)–O(10′)–P(11′)–O(12′)	−102.7(4)
C(9′)–O(10′)–P(11′)–O(13′)	18.9(4)
C(9′)–O(10′)–P(11′)–O(14′)	143.5(4)

double zwitterionic structure with N(15) and N(1′) atoms protonated and O(8′) and phosphate O(14′) atoms deprotonated. The carboxy group was in a neutral state with O(14) protonated. The phosphate takes the monoanionic form,[20] where the O(12′) is protonated with P–O = 1.546(6) Å. The bond angle of C(2′)–N(1′)–C(6′) [124.7(4)°] is characteristic of a pyridinium ring and is significantly larger than that of a neutral pyridine ring[21] (117.5°).

The indole and pyridinium rings are both planar to within ±0.04 and ±0.02 Å, respectively, and form a dihedral angle of 83.3(2)°. The tetrahydropyridine ring of β-carboline has a half-chair conformation with M helicity,[22] where the C(11) and N(15) atoms deviate by −0.324 and +0.397 Å, respectively, from a plane consisting of C(2), C(3) and C(10) and C(16) atoms, thus forming a distorted C(11)-*exo*–N(15)-*endo* conformation (Fig. 3). Similar ring puckering has frequently been observed in other synthetic tetrahydro-β-carbolines.[12,14]

One of the two hydrogen atoms attached to N(15) is intramolecularly hydrogen-bonded to the O(8′) atom of the pyridine ring [N(15)···O(8′) = 2.648(7) Å and N(15)–H(15)···O(8′) = 179.3(3)°]. The N(1) atom of the indole ring participates in two intramolecular hydrogen bonds with the phosphate O(14′) atom [N(1)···O(14′) = 3.074(7) Å and N(1)–H(1)···O(14′) = 136.1(3)°] and with the O(10′) atom [N(1)···O(10′) = 2.995(7) Å and N(1)–H(1)···O(10′) = 119.4(3) °]. Thus, the molecular conformation of **1** (Fig. 2) observed in the crystal structure is stabilized by these interactions, and the torsion angle around ω_1 is tightly fixed. The carboxy OH group is *anti* to the protonated N(15) atom with a torsion angle around O(14)–C(12)–C(11)–N(15) of 174.3(7)° and this conformation is determined by an electrostatic interaction between the O(13) and N(15) atoms [N(15)···O(13) 2.64(1) Å].

Solution Conformation.—In order to investigate whether or not the rigid conformation of **1** observed in the crystal structure is also kept in solution, ^{1}H NMR spectra of **1** were measured in DMSO solution. Chemical shifts and coupling constants for **1** are summarized in Table 3. The ROESY spectrum of H(11), H(16) and H(9′a and b) region is shown in Fig. 4. Since none of the NH and OH protons of **1** were observed in the DMSO solution, the electronic state (protonation or deprotonation) of **1** was not clear.

The vicinal coupling constants between C(10)H_2 and C(11)H (J 13.0 Hz for axial–axial and 4.0 Hz for equatorial–axial) suggest the half-chair C(11)-*exo*–N(15)-*endo* conformation[23–25] as the major conformation of the tetrahydropyridine ring of

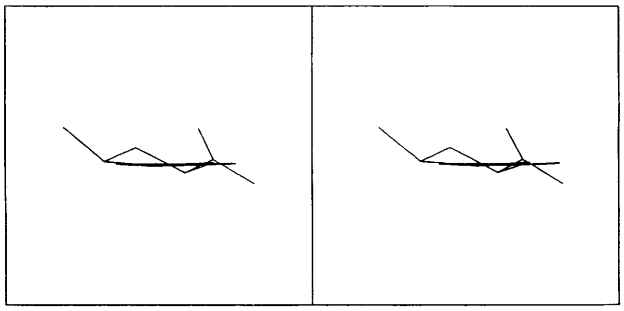

Fig. 3 Stereoscopic representation of the half-chair conformation of the tetrahydropyridine ring of β-carboline **1**, as viewed down the plane of the indole ring

Table 3 ^{1}H NMR chemical shifts (ppm), coupling constants (J/Hz) and possible angles[a] of **1** in [$^2H_6$]DMSO solution

Proton	Chemical shift	J/Hz	Possible φ angle (°)
H(4)	7.462 (br d, 1 H)	8.0 ($J_{4,5}$)	
H(5)	6.972 (ddd, 1 H)	8.0, 8.0, 1.0	
H(6)	7.019 (ddd, 1 H)	8.0, 8.0, 1.0	
H(7)	7.184 (br d, 1 H)	8.0 ($J_{7,6}$)	
$H(10)_{ax}$	2.881 (dd, 1 H)	13.0 ($J_{10ax,11ax}$)	−162 (−176)[b]
		15.0 ($J_{H10ax-H10eq}$)	
$H(10)_{eq}$	3.197 (dd, 1 H)	15.0 ($J_{10ax,10eq}$)	
		4.0 ($J_{H10eq-H11ax}$)	−55 (−29)
$H(11)_{ax}$	3.893 (dd, 1 H)	13.0 ($J_{11ax,10ax}$)	−162 (−176)
		4.0 ($J_{11ax,10eq}$)	−55 (−29)
H(16)	5.752 (s, 1 H)		
H(6′)	8.030 (s, 1 H)		
H(7′)	2.201 (s, 3 H)		
H(9′a)	5.089		
	(AB, 2 H)	16.0 ($J_{9'a,9'b}$)	
H(9′b)	5.108		

[a] φ corresponds to the torsion angle of H–C–C–H, calculated from $J_{vic} = 12.4\cos^2\varphi$ for $0 \leqslant \varphi \leqslant 90°$ and $J_{vic} = 14.3\cos^2\varphi$ for $90 \leqslant \varphi \leqslant 180°$.[25] Since these equations take no account of local charge and electronegativity effects which tend to reduce coupling constants, the observed $J_{ax,ax}$ (13.0 Hz) are about right for a φ value of ~180°. Similarly the $J_{eq,ax}$ of 4.0 Hz may fit the X-ray torsion angle of −29°, bearing in mind the reducing effects of the adjacent nitrogen and carboxyl groups. [b] The value in parentheses corresponds to the φ angle from the X-ray crystal structure analysis.

β-carboline (Table 3), the same as observed in the crystal structure (Fig. 3). This ring puckering was further suggested from the ROESY measurement. ROEs were clearly observed for the H(10)–H(11) and H(11)–H(16) proton pairs [Fig. 4(*a*)], suggesting a close disposition between the H(10) and H(11) and a parallel orientation between the C(11)–H(11) and C(16)–H(16) bonds.

As is obvious from Fig. 4(*b*), a notable ROE was observed between H(16) and either of the two H(9′) protons. This clearly reflects the predominant existence of a solution conformation similar to that observed in the crystal structure (see Fig. 2). Concerning the hydrogen bond in which the NH or OH proton participates, no NMR data were available. However, it would be reasonable to suppose that the proximity between H(16) and H(9′) is primarily due to the N(15)–H···O(8′) intramolecular hydrogen bond. In conclusion, it appears that the preferred conformation for **1** in DMSO solution is very similar to that observed in the crystal structure.

Molecular Orbital Calculations.—The conformational analysis of **2**, a model compound which substitutes an OH group for the phosphate group of **1**, was carried out by CNDO/2 calculations. The two torsion angles ω_1 and ω_2 were rotated in

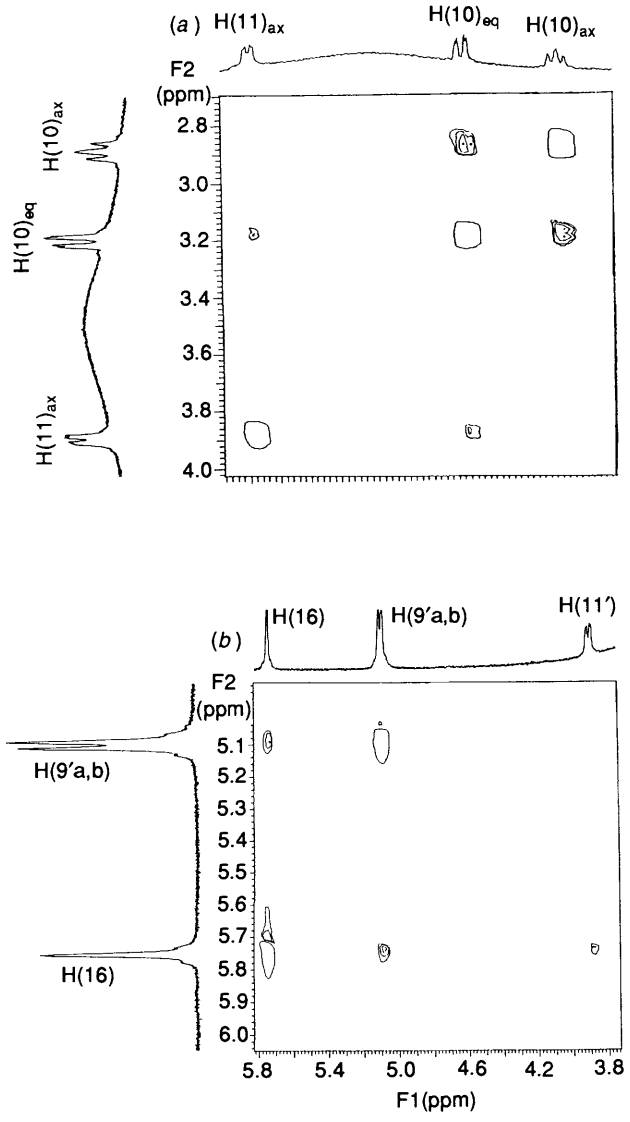

Fig. 4 Partial ROESY spectrum of (*a*) the H(10) and H(11) region and (*b*) the H(11), H(16) and H(9'a and 9'b) region. Mixing time = 200 ms.

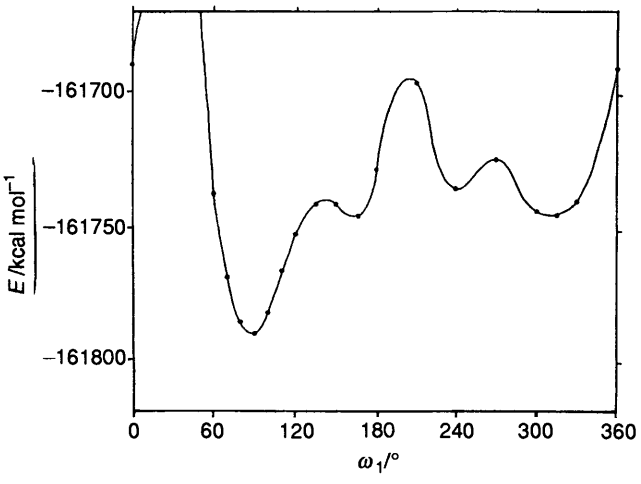

Fig. 5 Energy profile of **2** as a function of ω_1. The ω_2 value is set to the value giving the lowest energy for each conformer of ω_1.

increments of 30° from 0 to 360°. Using the most stable conformer obtained, the energy calculations were continued with intervals of 10° in the range of ±30°. Fig. 5 shows the variation the total energy of **2** as a function of ω_1, where ω_2 is set to the value giving the lowest energy for each conformer of ω_1. It

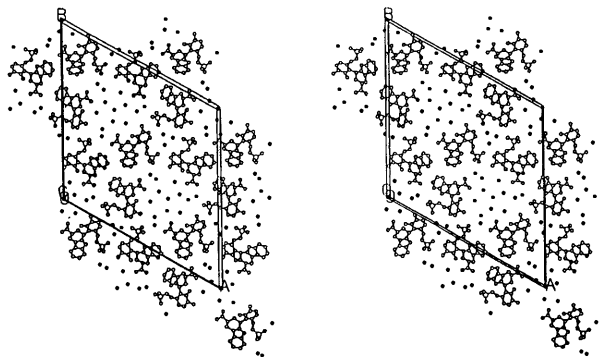

Fig. 6 A stereoscopic view of the crystal packing of **1**, viewed down the *c*-axis. Filled circles represent water molecules of crystallization.

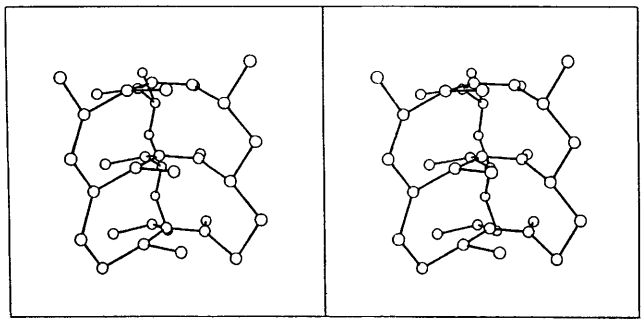

Fig. 7 A stereoscopic view of the hydration shell created by the packing of the water molecules viewed perpendicular to the three-fold symmetry axis. The shell is elongated along the *c*-axis.

was assumed that $\omega_1 = 60 \sim 130°$ gave the predominant form ($\omega_1 = 90$, $\omega_2 = -60°$ for the most stable conformer) and the energy difference from the second most stable conformer ($\omega_1 = 270 \sim 360°$) was 46.0 kcal mol^{-1} (1 cal = 4.184 J). This can be interpreted as being the result of an electrostatic (or hydrogen-bonded) interaction between the N-15 and O-8' atoms. The slight deviation of the molecular conformation of **1** in the crystal structure ($\omega_1 = 105.9$, $\omega_2 = -58.9°$) from the most stable conformer of **2** is due to the further participation of a hydrogen bond between the phosphate oxygen atom and indole NH group and to the crystal packing effect among the neighbouring molecules. To take account of the electronic state of **1** under physiological conditions ($pK_a = 4.10$ and 8.57 for pyridoxal, and $pK_a = 2.38$ and 9.39 for tryptophan), the chemical structure of **2** with O-14 deprotonated and N-15 protonated was also subjected to CNDO/2 conformational analysis. As a result, nearly the same energy profile as shown in Fig. 5 was obtained, and the conformer of $\omega_1 = 90°$ and $\omega_2 = -60°$ was taken to be the most stable.

Judging from the solid-state, solution and molecular orbital studies described, it can be concluded that **1** takes a preferred conformation where the indole ring of β-carboline and the pyridine ring of PLP are almost at right angles to each other; the conformation being mainly stabilized by a N(15)···O(8') intramolecular hydrogen bond.

Crystal Structure of **1** *and Hydrogen Bonds.*—A stereoscopic view of crystal structure, viewed along the *c*-axis, is shown in Fig. 6, where filled circles represent water of crystallization. Possible hydrogen bonds and short contacts of less than 3.4 Å are presented in Table 4. One of the most characteristic features in the crystal structure is the hydrogen bonding pattern of the water of crystallization. Thirteen water molecules, one of which [O(6)W] is located on the three-fold symmetry axis and the

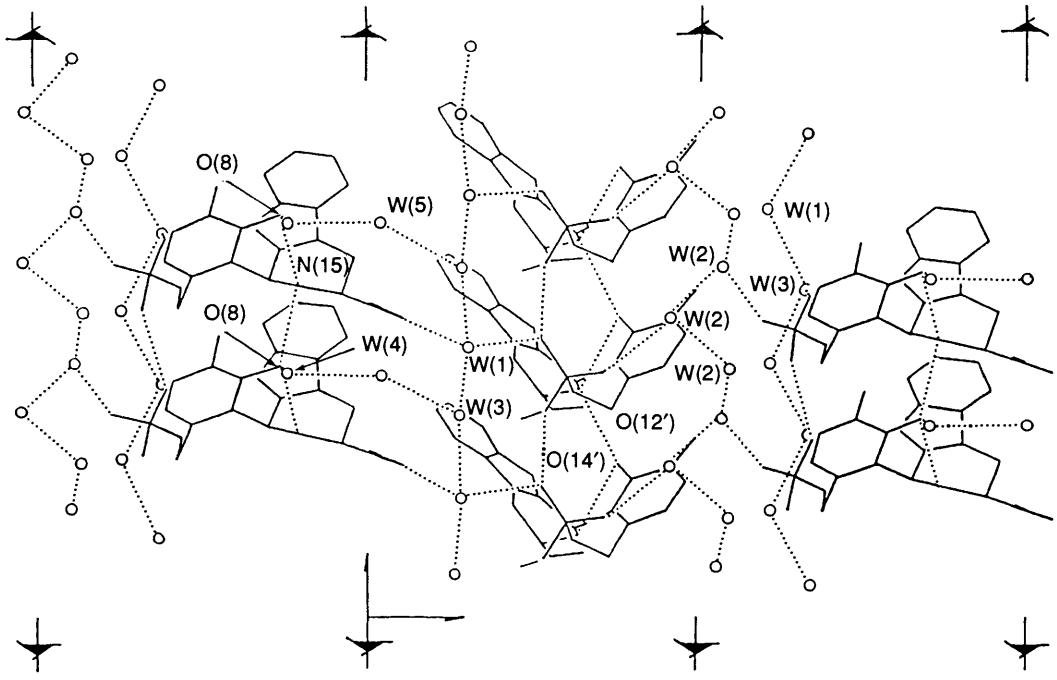

Fig. 8 Schematic view of hydrogen bonding network formed between **1** and the water molecules. Open circles indicate water molecules and dotted lines represent hydrogen bonds.

Table 4 Hydrogen bonds and short contacts (< 3.4 Å)

Donor (D)	Acceptor (A)	Symmetry operation	D···A (Å)
Hydrogen bond			
N(1)	O(14')	x,y,z	3.074(7)
O(14)	O(1)W	$-y + 5/3, x - y + 1/3, z - 2/3$	2.61(1)
N(15)	O(8')	x,y,z	2.648(7)
N(15)	O(8')	$x,y,z - 1$	2.753(7)
N(1')	O(13')	$-x + y + 2/3, -x + 4/3, z + 1/3$	2.645(6)
O(12')	O(14')	$x,y,z - 1$	2.576(7)
O(1)W	O(14')	x,y,z	2.838(9)
O(1)W	O(3)W	x,y,z	2.79(2)
O(2)W	O(13')	x,y,z	2.73(1)
O(2)W	O(2)W	$-x + y + 2/3, -x + 4/3, z + 1/3$	2.59(1)
O(3)W	O(1)W	$x,y,z - 1$	2.89(2)
O(3)W	O(5)W	$-x + y + 4/3, -x + 5/3, z - 1/3$	2.65(9)
O(4)W	O(8')	x,y,z	2.91(4)
O(4)W	O(5)W	x,y,z	3.0(1)
O(5)W	O(6)W	$x + 2/3, y + 1/3, z + 1/3$	2.68(9)
Short contact			
N(1)	O(10')	x,y,z	2.995(7)
N(15)	O(13)	x,y,z	2.64(1)
C(16)	O(8')	$x,y,z - 1$	3.320(7)
C(4')	O(10')	x,y,z	3.020(7)
C(6')	O(13')	$-x + y + 2/3, -x + 4/3, z + 1/3$	3.370(8)
C(6')	O(2)W	$-x + y + 2/3, -x + 4/3, z - 2/3$	3.23(1)

remaining are related to one another by the symmetry, are located in a large cavity which is created by the molecular packing of **1**. The packing of the water molecules into this cavity appears to be relatively loose as shown by their high thermal parameters. However, their packing pattern is reasonable and forms a three-dimensional hydrogen-bonded network (hydration shell) elongated along the *c*-axis (Fig. 7).

The hydrogen bonding network formed between **1** and the water molecules is shown schematically in Fig. 8, which corresponds to a part of the packing layer along the (020) or (200) plane. The molecules stacked along the *c*-axis are linked by two hydrogen bonds, O(12')–H···O(14') and N(15)–H···O(8'), thus forming an infinite layer. The water molecules are located among these layers, related by 3_1 symmetry, and link the layers by two or three hydrogen bonds.

References

1 *Vitamin B6, Pyridoxal Phosphate, Chemical, Biochemical and Medical Aspects*, eds. D. Dolphin, R. Poulson and O. Avramovic, Wiley, New York, 1986, part B.
2 H. C. Dunathan, in *Advances in Enzymology*, ed. A. Meister, Wiley, New York, 1971, vol. 35, pp. 79–134.
3 D. Heyl, S. A. Harris and K. Folkers, *J. Am. Chem. Soc.*, 1948, **70**, 3429.
4 Y. Matsushima, *Chem. Pharm. Bull.*, 1968, **16**, 2046.
5 H. F. Schott and W. G. Clark, *J. Biol. Chem.*, 1952, **196**, 449.
6 K. Wohl and Cz. Maslinski, *Agents Actions*, 1975, **5**, 20.
7 K. Sasiak, D. Kierska, M. Boguslawski and Cz. Maslinski, *Agents Actions*, 1975, **5**, 25.
8 D. Kierska and Cz. Maslinski, *Agents Actions*, 1975, **5**, 471.
9 N. S. Buckholz and W. O. Boggan, *Biochem. Pharmacol.*, 1969, **25**, 1423.
10 S. F. Contractor and M. K. Jaacock, *Biochem. Pharmacol.*, 1967, **16**, 1981.
11 R. J. Gryglewski, S. Misztal, J. A. Splawinski and B. Panczenko, *J. Med. Chem.*, 1966, **6**, 471.
12 F. Ungemach, D. Soerens, R. Weber, M. DiPierro, O. Campos, P. Mokry, J. M. Cook and J. V. Silverton, *J. Am. Chem. Soc.*, 1980, **102**, 6976.
13 J. Liu, M. Nakagawsa and T. Hino, *Tetrahedron*, 1989, **24**, 7729.
14 W. J. Colucci, L. Tilstra, M. C. Sattler, F. R. Fronczek and M. D. Barkley, *J. Am. Chem. Soc.*, 1990, **112**, 9182.
15 N. Walker and D. Stuart, *Acta Crystallogr., Sect. A*, 1983, **39**, 158.
16 T. Debaerdemaeker, G. Germain, P. Main, C. Tate and M. M. Woolfson, MULTAN87, a System of Computer Programs for the Automatic Solution of Crystal Structures from X-ray Diffraction Data, Universities of York, England and Louvain, Belgium, 1987.
17 G. M. Sheldrick, SHELX76, Program for crystal structure determination, University of Cambridge, England, 1976.
18 *The Universal Crystallographic Computing System-Osaka*, The Computation Center, Osaka University, Osaka, Japan, 1979.
19 *International Tables for X-ray Crystallography*, Kynoch Press, Birmingham, England, 1974, vol. 4.
20 W. Saenger, *Principles of Nucleic Acid Structure*, Springer-Verlag, New York, 1984, pp. 51–104.

21 M. Inoue, T. Sakaki, T. Fujiwara and K. Tomita, *Bull. Chem. Soc. Jpn.*, 1978, **51**, 1118.
22 L. Casella and M. Gullotti, *J. Am. Chem. Soc.*, 1981, **103**, 6338.
23 M. Karplus, *J. Am. Chem. Soc.*, 1963, **85**, 2870.
24 N. S. Bhacca and D. H. Williams, in *Application of NMR Spectroscopy in Organic Chemistry*, Holden-Day, San Francisco, 1964, ch. 6.
25 R. J. Abraham and J. E. S. Holker, *J. Chem. Soc.*, 1963, 806.

Paper 3/07366A
Received 14*th December* 1993
Accepted 31*st January* 1994